Ray & Redkar, *Cogent Engineering* (2014), 1: 988402
http://dx.doi.org/10.1080/23311916.2014.988402

cogent engineering

MECHANICAL ENGINEERING | RESEARCH ARTICLE

Analysis and simulation of Wiseman hypocycloid engine

Priyesh Ray[1] and Sangram Redkar[1*]

Received: 28 March 2014
Accepted: 12 November 2014
Published: 16 December 2014

*Corresponding author: Sangram Redkar, Department of Engineering, Arizona State University, Mesa, AZ 85212, USA
E-mail: sredkar@asu.edu

Reviewing editor:
Duc Pham, University of Birmingham, UK

Additional information is available at the end of the article

Abstract: This research studies an alternative to the slider-crank mechanism for internal combustion engines, which was proposed by the Wiseman Technologies Inc. Their design involved replacing the crankshaft with a hypocycloid gear assembly. The unique hypocycloid gear arrangement allowed the piston and connecting rod to move in a straight line creating a perfect sinusoidal motion, without any side loads. In this work, the Wiseman hypocycloid engine was modeled in a commercial engine simulation software and compared to slider-crank engine of the same size. The engine's performance was studied, while operating on diesel, ethanol, and gasoline fuel. Furthermore, a scaling analysis on the Wiseman engine prototypes was carried out to understand how the performance of the engine is affected by increasing the output power and cylinder displacement. It was found that the existing 30cc Wiseman engine produced about 7% less power at peak speeds than the slider-crank engine of the same size. These results were concurrent with the dynamometer tests performed in the past. It also produced lower torque and was about 6% less fuel efficient than the slider-crank engine. The four-stroke diesel variant of the same Wiseman engine performed better than the two-stroke gasoline version. The Wiseman engine with a contra piston (that allowed to vary the compression ratio) showed poor fuel efficiency but produced higher torque when operating on E85 fuel. It also produced about 1.4% more power than while running on gasoline. While analyzing effects of the engine size on the Wiseman hypocycloid engine prototypes, it was found that the engines performed better in terms of power, torque, fuel efficiency, and cylinder brake mean effective pressure as the displacement increased. The 30 horsepower (HP) conceptual Wiseman prototype, while operating on E85, produced the most optimum results in all aspects, and the diesel test for the same engine proved to be the most fuel efficient.

Subjects: Energy & Fuels; Mechanical Engineering; Mechanical Engineering Design

Keywords: hypocycloid engine; multi-fuel analysis

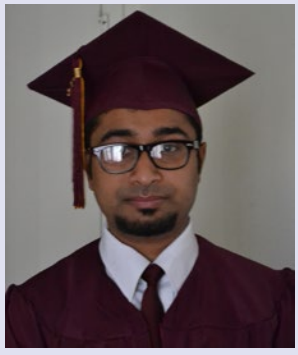

ABOUT THE AUTHORS

Priyesh Ray graduated with Master of Science in Technology from Arizona State University in 2014. He completed his Bachelor's from Arizona State University in 2012. His research interests are engine design and testing.

Sangram Redkar is an associate professor in Polytechnic School at Arizona State University. He completed his PhD from Auburn University in 2005. His research interests are robotics, dynamics and control, and machine design.

PUBLIC INTEREST STATEMENT

This research investigates a performance, multi-fuel operation and scalability of a hypocycloid engine. This engine is based on Wiseman hypocycloid mechanism. In this engine, connecting rod motion is purely translational that minimizes the size loads and corresponding frictional losses observed in a typical slider-crank engine. The advantages and disadvantages of this hypocycloid engine along with simulation and experimental data are presented in this paper.

1. Introduction

Internal combustion engines (ICEs) have been around for centuries and the slider-crank mechanism is typically used to convert the reciprocating motion of piston to rotary motion of crankshaft. Despite its popularity, the slider-crank mechanism still has a few flaws, for example the higher side load and associated frictional losses in the piston cylinder assembly. Wiseman Technologies Inc (WTI) proposed an alternate mechanism as a solution to tackle this problem in the form of Wiseman hypocycloid engine (WHE). It consists of a unique gear assembly based on the hypocycloid concept.

As shown in Figure 1, a hypocycloid is a curve produced by tracing the fixed point "*P*" on the circumference of the small circle (of radius r_a), as it rolls inside the large circle (of radius r_b). The path of that curve is given by the following equations;

$$x = (r_a - r_b)\cos\emptyset + r_b \cos\left(\frac{r_a - r_b}{r_b}\emptyset\right) \tag{1}$$

$$y = (r_a - r_b)\sin\emptyset - r_b \sin\left(\frac{r_a - r_b}{r_b}\emptyset\right) \tag{2}$$

where r_a is the radius of the smaller circle; r_b is the radius of the larger circle; $\emptyset$ is the angle from the *x* axis to the line that intersects the center of circle "*a*" and circle "*b*".

Now, in a special case, where the ratio of the radii of the two circles is 2:1, the hypocycloid curve at any given point on the circumference of circle "*b*" is a straight line. When the circles are replaced by gears, whose pitch diameters have a ratio of 2:1, then such an assembly can be used to produce a perfect straight-line motion of a piston in an ICE. In Figure 2, the smaller pinion gear in red can be compared to the small circle "*a*" and the internal ring gear (blue) to the larger circle "*b*" in Figure 1. The visualization shows that a specific point on the pitch diameter of the pinion gear is always coincident with the vertical black line, as it rolls inside the ring gear. The black line indicates the path of the piston and the connecting rod.

Historically, the hypocycloid engine variants have received some attention from the scientific community. Many patents have been filed around the hypocycloid mechanism and its application to pump, compressors, and engines. In 1802, Murray used the hypocycloid mechanism to build a steam engine (Karhula, 2008). In 1975, Ishida published an excellent paper that focused on the inertial shaking forces and moments of a hypocycloid engine and compared to a conventional slider-crank

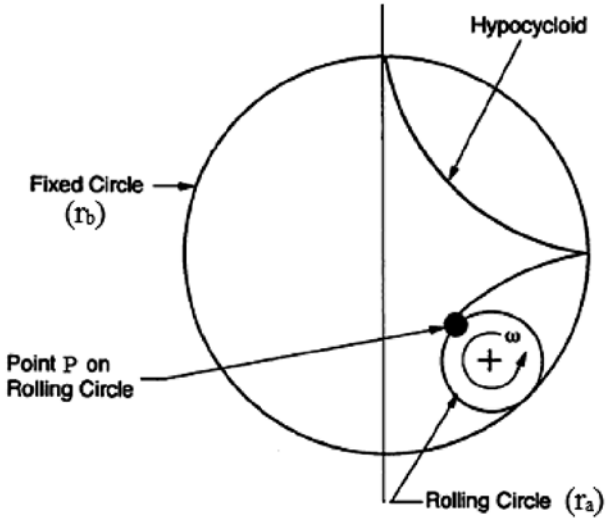

Figure 1. Hypocycloid concept (*Special plane curves*, 2005–2014).

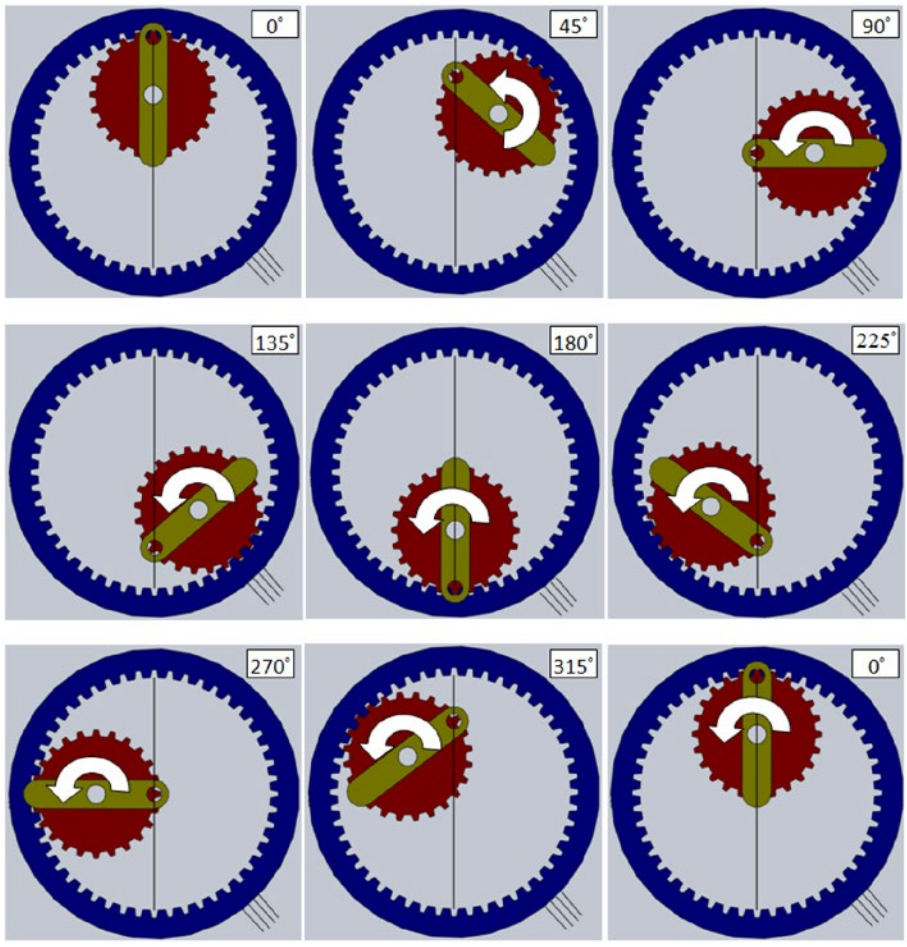

Figure 2. Geared hypocycloid concept rotating at 45° increments (Conner, 2011).

engine (Ishida & Matsuda, 1975). Building upon Ishida's research, Drs. Beachley and Lenz published a paper that proposed an interesting method to attain perfect balance in hypocycloid engines (Beachley & Lenz, 1988).

Another important contribution to the study of hypocycloid engine came from Drs. Ruch, Fronczak, and Beachley (1991). They studied a variant of hypocycloid engine called the modified hypocycloid engine. This engine had a third gear that reduced the overall individual gear tooth loads. In 1998, Andriano designed and tested of a full crank 125cc two-stroke hypocycloid engine (Andriano, 1998). Their design had a seal around the connecting rod to isolate the crankcase from the top end. In 2008, Karhula published a paper that compared slider-crank and hypocycloid engines of equal dimensions (stroke, bore, etc.) (Karhula, 2008). For more details and a detailed literature review, the reader is referred to the thesis by Conner (2011).

Though a simple hypocycloid mechanism such as Cardan Gear produces a straight line with a perfect sinusoidal motion at any given point, the angle of the straight line depends on the point selected on the pitch of the small pinion gear. WTI modified this gear assembly and incorporated it in their hypocycloid engine, which was patented in 2001. The first WHE was built by adding a link to support the pinion gear where the rotating motion of the gear is transferred to a rotating output shaft (L2) as shown in Figure 3. The point D1 as seen in Figure 3 was connected to the bottom end of the connecting rod. This point represented the point "*P*" shown in Figure 1.

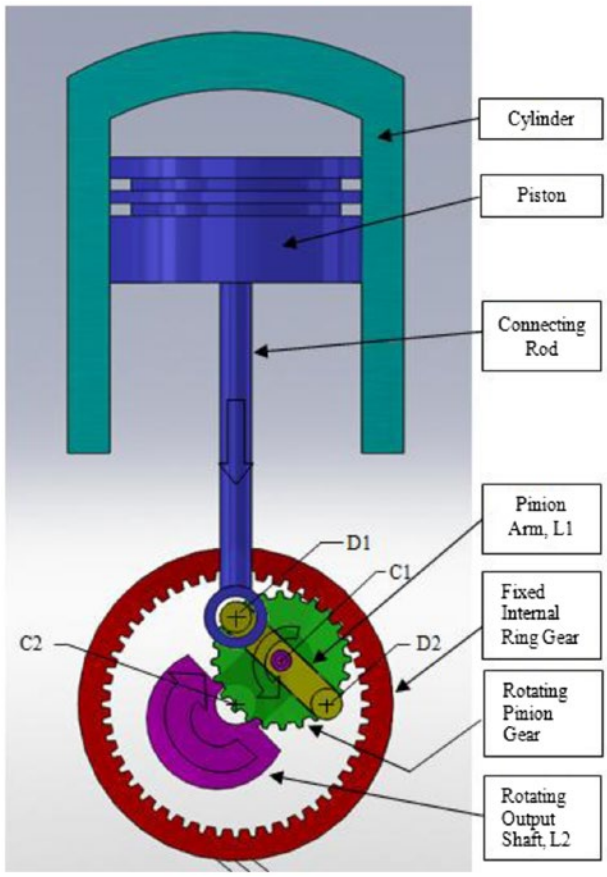

Figure 3. Wiseman gear and connecting rod assembly (Conner, 2011).

The proposed link in the Wiseman mechanism (Wiseman, 2001) to support the pinion gear (Item 200), known as the carrier shaft (Item 100), can be seen in Figure 4. The Wiseman mechanism also has a provision for the pinion gear teeth (Item 204) to mesh with the fixed internal ring gear (Item 6) in the form of a cavity (Item 322). This unique mechanical assembly allowed the piston in the Wiseman engine to travel in a perfect straight line sinusoidal motion eliminating any piston side load (Wiseman Engine Group, 2010). It also eliminated connecting rod bending and reduced the engine heat loss due to side load friction.

The conceptual Wiseman Engine is shown in Figure 5(a). As discussed earlier, the path of the crankpin in the Wiseman engine is hypocycloidal instead of circular. This provides the advantages such as longer power stroke, straight line motion better performance, and less wear.

2. Software simulations

To analyze the performance of the WHE, the Lotus Engine Simulation (LES) software was extensively used. The LES software is capable of simulating the performance of an ICE and can predict various output parameters of engine under different operating conditions. These parameters can be fuel efficiency, power output, torque, and running temperature of the engine over a period of time. Before trying a completely new hypocycloid engine concept in LES, the authors decided to validate the LES simulation results for a conventional slider-crank four-stroke (GUNT 1B30) diesel engine that was available in our laboratory. The GUNT engine is a four-stroke, single cylinder, air-cooled engine, with direct injection that works on both diesel and biodiesel fuels. The compression ratio for this engine is 21.5 with a mean piston speed of 6.9 m/s and a mechanical efficiency of 87%. For GUNT 1B30 engine, a model was created in LES with specifications as shown in Table 1. The software simulations were

Figure 4. Patented Wiseman design (Wiseman, 2001).

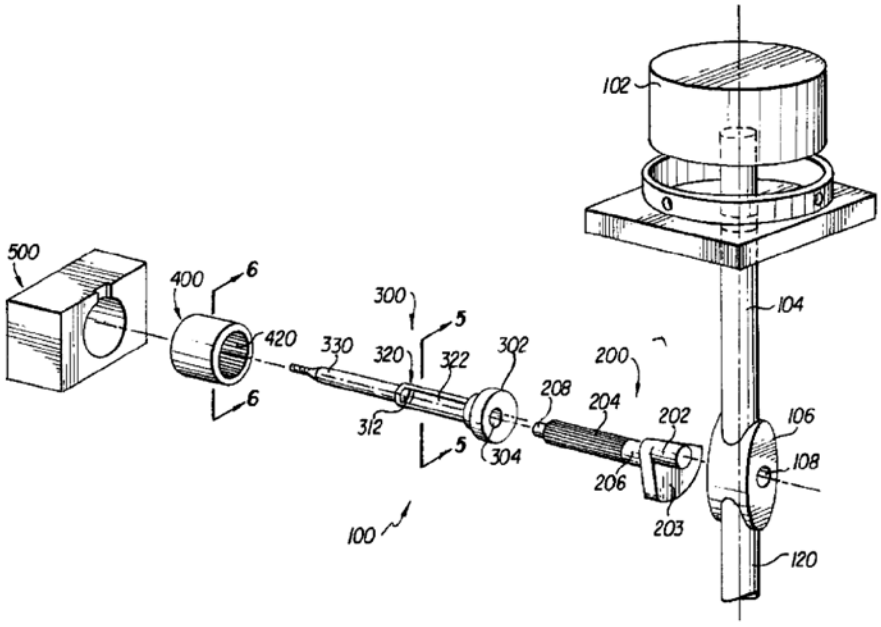

Figure 5(a). Wiseman engine conceptual model (Conner, 2011).

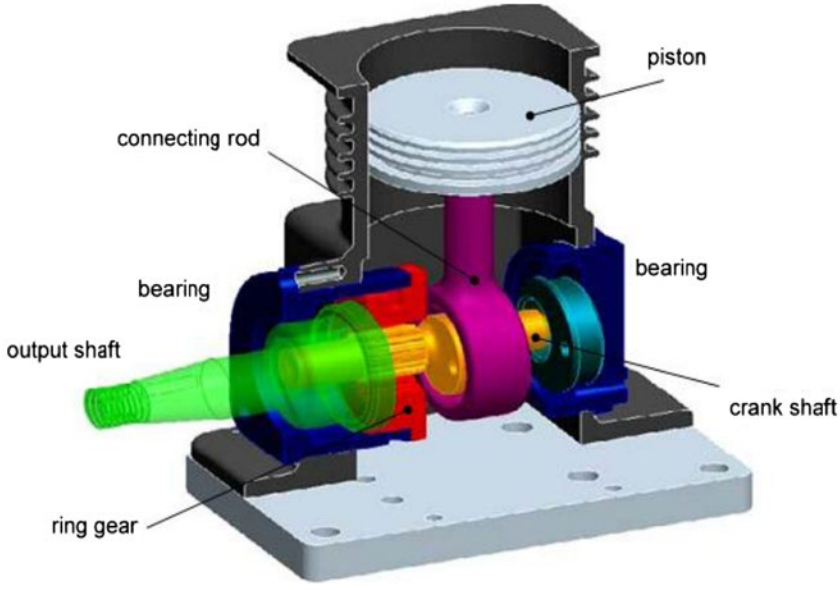

Table 1. GUNT 1B30 engine specifications (Hatz Diesel, 2012)

Power	Stroke	Bore Ø	Displacement
5.5 KW @ 3,500 rpm	69 mm	80 mm	347cc

carried out to obtain performance results. These software results were compared to manufacturer supplied performance data. Furthermore, to validate the authenticity of the results, the simulation results were compared with dynamometer test data.

Figure 5(b). LES results for GUNT engine.

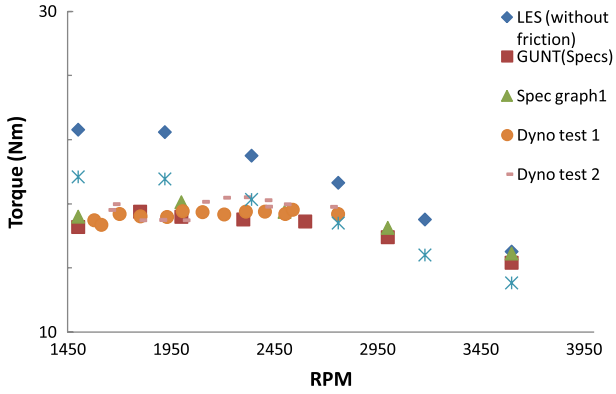

Figure 5(b) shows the LES simulation results (with and without the frictional/mechanical losses), manufacturer supplied performance plots, and experimental (dynamometer testing) results. The GUNT engine has the mechanical efficiency of 87%. LES (without friction) assumed mechanical efficiency as 100%. These LES (without friction) results were then multiplied later with 0.87 to compensate for the mechanical efficiency and called LES (with friction). It can be noticed in Figure 5(b) that the torque results recorded during the dynamometer tests coincided very well with the manufacturer specifications at 2,500–3,000 rpm. The slight variation in simulated and actual results can be observed because a perfect displacement scavenging model was selected for the simulation, which assumes that all the residual gases are removed, and only a fresh charge of air is present during the combustion. But otherwise, the LES software results are comparable to the test and manufacturer data, and show the same trend.

2.1. Modeling the Wiseman engine

Once the reliability of the LES software was established for a conventional slider-crank engine, it was used to model the WHE 30cc prototype. The Wiseman engine prototype is 30cc, two-stroke, single cylinder, with spark ignited and carbureted fuel system. It is designed to generate 0.99 HP of power at around 7,000 rpm. To model the engine in LES software, an intake disk valve was also used in addition to variable volume inlet plenum. Wiseman engine has piston ported intake and exhaust valves with dimensions shown in Table 2.

This Wiseman engine prototype was built from a 30cc weed-wacker slider-crank engine, where the slider-crank mechanism was replaced with Wiseman hypocycloid mechanism. Table 3 provides a summary of their respective design specifications.

Table 2. Wiseman LES port data

	Intake	Exhaust
Port width (mm)	40	20.82
Maximum port height (mm)	2	7.41
Valve open (°)	124	108

Table 3. Summary of Wiseman and stock engine cylinder dimensions

Engine	Stroke	Bore Ø	Displacement
Wiseman engine	1.125 in (28.6 mm)	1.435 in (36.5 mm)	1.819 in^3 (29.81cc)
Stock homelite	1.114 in (28.3 mm)	1.435 in (36.5 mm)	1.802 in^3 (29.53cc)

The intake and exhaust pipe geometry in the software model was assumed to be simple tubes of approximate dimensions of the carburetor nozzle, at wide-open position. A single Wiebe combustion model was used for combustion analysis. This model assumes that the heat released during the combustion heats the whole combustion chamber.

The single Wiebe function defines the mass fraction burned as:

$$1 - \exp^{-A\left(\frac{\theta}{\theta_b}\right)^{M+1}} \tag{3}$$

where the Wiebe coefficients *A* and *M* for gasoline are 10.0 and 2.0, respectively.

A simpler, Annand heat transfer model (Annand, 1963) was used for the Wiseman engine which was given by:

$$\frac{hD}{k} = ARe^{B} \tag{4}$$

where *h* is the heat transfer coefficient; *A* and *B* are the Annand open or close cycle coefficients; *K* is the thermal conductivity of gas in the cylinder; *D* is the cylinder bore diameter; *Re* is the Reynolds number based on the means piston speed and engine bore (The *A* and *B* coefficients for a carbureted or a port injected combustion system are 0.2 and 0.8, respectively.).

One of the key characteristics of the Wiseman engine is its hypocycloid mechanism. The LES software assumes that all the engines models designed in it follow the piston motion of a slider-crank engine, and so the results are simulated accordingly. To simulate the Wiseman engine according to the hypocycloid piston motion, a user specific subroutine was created. The equations in the subroutine were based on the piston motion equations of the Wiseman hypocycloid gear train, which provided the instantaneous position and the cylinder volume, while the piston is in the motion. These equations were derived from Figure 6.

The distance *P* or piston position is relative to the Top Dead Center (TDC). After finding the piston postion, the volume is found by using:

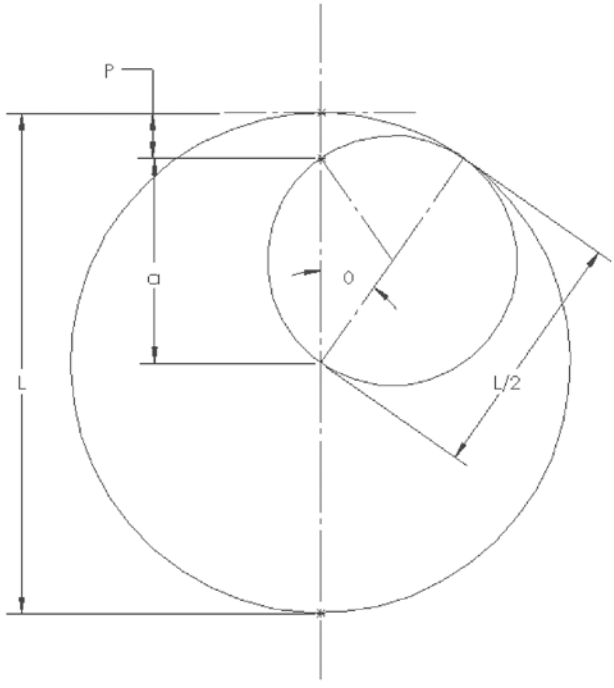

Figure 6. Wiseman (hypocycloid) piston position diagram.

$$P = \frac{L}{2} - \left(\frac{L}{2}\cos\theta\right) \tag{5}$$

$$V' = P\left(\frac{\pi B^2}{4}\right) \tag{6}$$

where L is the stroke of the engine; θ is the crank angle with 0° being TDC; V' is the volume above piston, TDC being 0; B is the diameter of the cylinder (bore); P is the position of the piston with the origin being TDC.

It was also known that the the volume of the Wiseman engine at each crank angle is lower than that of the original stock engine since its piston sits higher than the stock engine. This provides less combustion volume at each crank angle. Previous dynamometer tests on the Wiseman engine suggested that the engine operates at a mechanical efficiency of 60.6%, and this was taken into consideration while modeling the engine friction. Furthermore, a virtual sensor was attached to the cylinder block in the LES model to record the crank angle, piston speed, and position, as seen in Figure 7.

To verify the modification in the piston motion, the model was simulated using subroutines for a conventional slider-crank and the WHE. The data collected from the sensor for both the runs was recorded and compared to see the change in the piston movement, which can be seen in Figures 8 and 9.

From Figure 8, it was noticed that the piston velocity for a slider-crank engine does not trace a perfect cosine–time curve, whereas the hypocycloid piston motion syncs perfectly with the cosine curve. There is nonlinearity in the slider-crank mechanism, and so the piston motion is not a harmonic function. Similar observation can be made from Figure 9, the displacement of hypocycloid engine is harmonic but the displacement of the slider-crank engine is not.

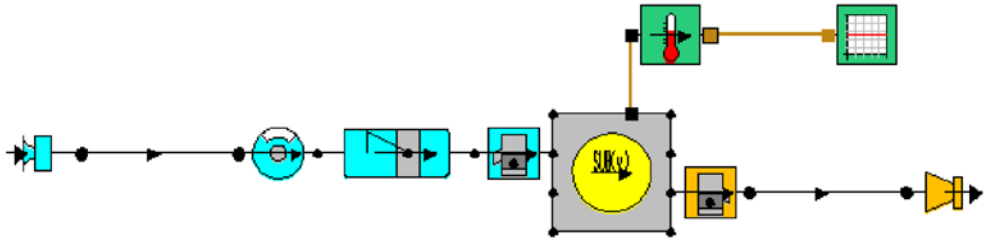

Figure 7. LES model of Wiseman engine.

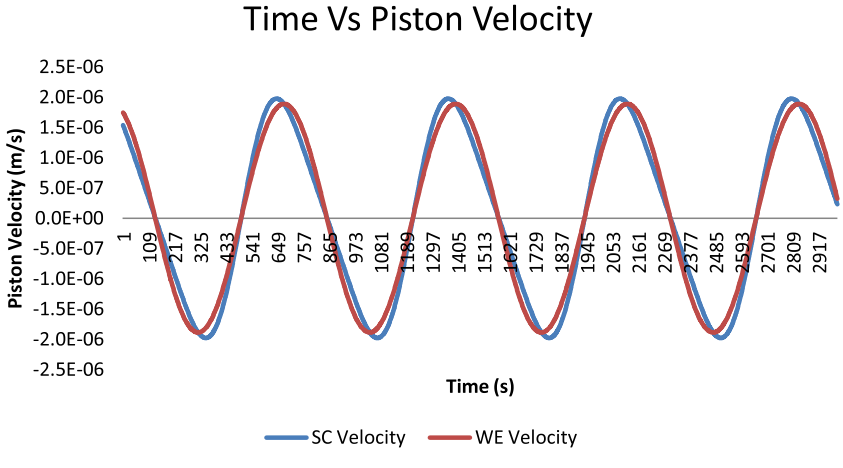

Figure 8. Comparison of time vs. piston velocity of slider-crank (SC) and Wiseman engine (WE).

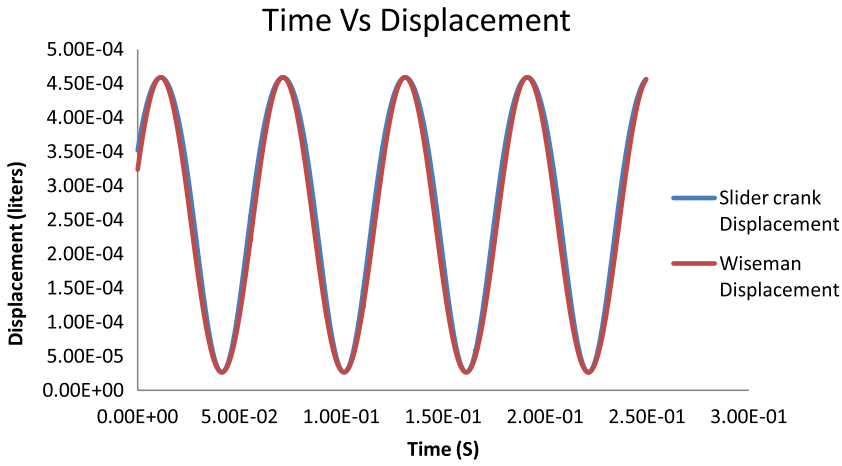

Figure 9. Comparison of time vs. displacement volume of slider-crank and Wiseman engine.

2.2. Comparison of simulation with experiments

As mentioned earlier, a weed-wacker engine was modified to incorporate Wiseman hypocycloid mechanism. This prototype engine was termed WHE alpha prototype. It is a 30cc two-stroke, single cylinder engine that is designed to produce 1 HP. This engine was modeled in LES software, and simulated for speeds ranging from 1,000 to 8,000 rpm with an increment of 1,000 rpm. A similar commercially available slider-crank engine was also simulated in LES software under identical conditions. The results from the simulations are shown in Figures 10–12.

As seen in Figure 10, the Wiseman engine at 6,000 rpm produced slightly less power than the slider-crank engine. Its power output at 6,000 rpm was 0.62 KW (0.83 HP), and the same for the slider-crank engine was 0.66 KW (0.89 HP). Similar trend can be observed as the engine RPM increased. At all speeds, slider-crank engine of 30cc capacity produced more power compared to the Wiseman engine.

Furthermore, comparing the software results for output torque of both the engines, it can be seen from Figure 11 that the torque at peak RPM of Wiseman engine is slightly less than that of the slider-crank at the same RPM. This could be because the Wiseman engine has a shorter stroke length than the slider-crank engine. The Wiseman engine at 6,000 rpm produces 0.98 Nm of torque, and the slider-crank engine produces 1.05 Nm. Similar trend can be observed as the engine RPM increased. At all speeds, slider-crank engine of 30cc capacity produced more torque compared to the Wiseman engine.

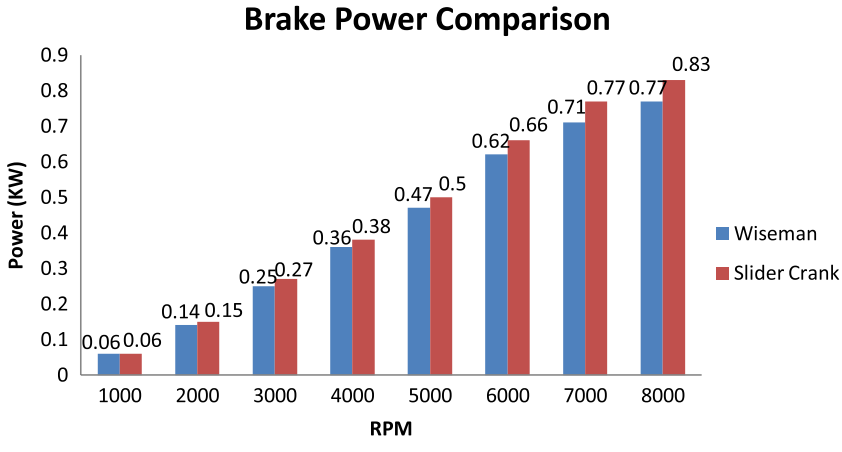

Figure 10. LES results of Wiseman and slider-crank engine for brake power.

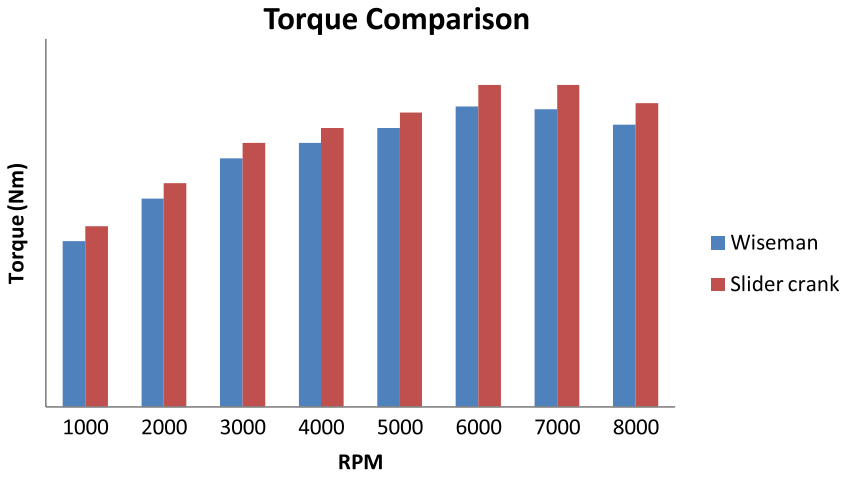

Figure 11. LES results of Wiseman and slider-crank engine for torque.

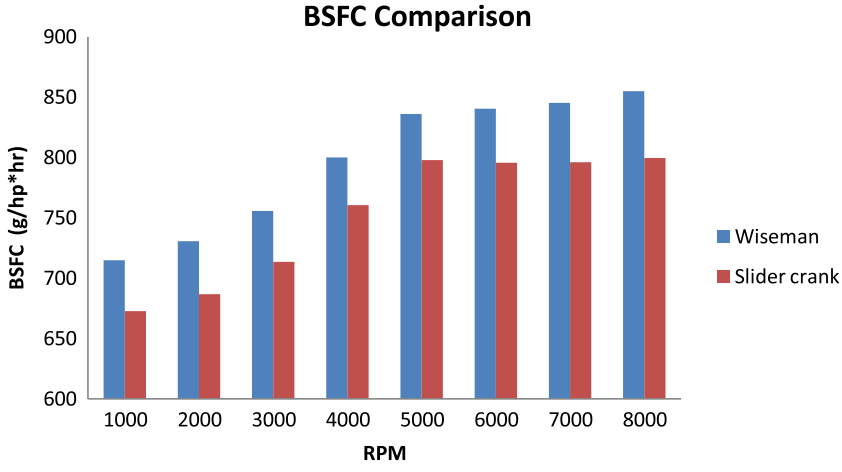

Figure 12. LES results of Wiseman and slider-crank engine for BSFC.

As shown in Figure 12, it can be noted that the Wiseman engine at 6,000 rpm resulted in a break specific fuel consumption (BSFC) of 840.42 g/hp h, while the slider-crank engine returned to 795.5 g/hp h. This shows that the Wiseman engine is about 6% less fuel efficient than the slider-crank engine. It can be observed that all speeds slider-crank engine of 30cc capacity has less BSFC compared to Wiseman engine.

The WHE alpha prototype was tested using a dynamometer at MTD Southwest Inc. in Chandler, Arizona. During the dynamometer tests, the WHE alpha prototype engine's performance was also compared to that of a commercial slider-crank (MTD) engine of the same size. A brief summary of these results can be seen in Table 4.

In the dynamometer tests, it was observed that at a peak speed of 7,000 rpm, the Wiseman engine had about 5% higher loss in power than a stock engine of the same size. The Wiseman engine was also found to be 21% less fuel efficient compared to a slider-crank engine at 6,000 rpm. The trend of higher BSFC in the Wiseman engine is concurrent with the results from the dynamometer tests.

Table 4. Wiseman dynamometer test summary (Conner, 2011)

Engine	Peak power	BSFC
MTD engine (31cc)	0.96 HP @ 7,000 rpm	410.08 g/hp h
Wiseman engine	0.60 HP @ 6,000 rpm	520.06 g/hp h

3. Multi-fuel and scaling of WHE

To explore the range of applications of the Wiseman engine, it was necessary to analyze its performance while operating on different fuels. For the same purpose, a four-stroke diesel variant of the Wiseman engine was modeled and simulated in LES. To simulate a four-stroke diesel Wiseman engine, the existing LES software model for the 30cc two-stroke engine was modified. The physical parameters of the engine such as the bore and stroke dimensions, swept volume, and connecting rod length were kept unchanged, but the compression ratio was increased from 8:1 to 17:1. Also, the fuel delivery system was changed to direct injection type instead of carbureted. The engine results were then simulated under the similar test conditions as the original gasoline engine. The results for engine's output power, torque, and fuel consumption can be seen in the following plots.

From the data in Figures 13–15, it can be noticed that the four-stroke diesel Wiseman engine performed better than both the two-stroke Wiseman engine (using gasoline) and the two-stroke slider-crank engine. This improvement in the performance was consistent for power (Figure 13), torque (Figure 14), and fuel consumption (BSFC) at peak RPMs (Figure 15). The improvement can be credited to the higher volumetric efficiency of the four-stroke engine, which reduced the loss of air–fuel mixture during the combustion resulting in better fuel efficiency (Ganesan, 2012, p. 638). The proper utilization of the air in the four-stroke engine also resulted in increased power output. Furthermore, the absence of piston ports increased the effective cylinder fuel compression range in the four-stroke engine (Table 5).

WTI (n.d.) has also proposed a VCR-Variable Compression engine to be used in an Unmanned Arial Vehicle (UAV). The engine's design incorporated an adjustable contra piston which enables the operator to change the engine's compression ratio while it is running. This engine has a modified

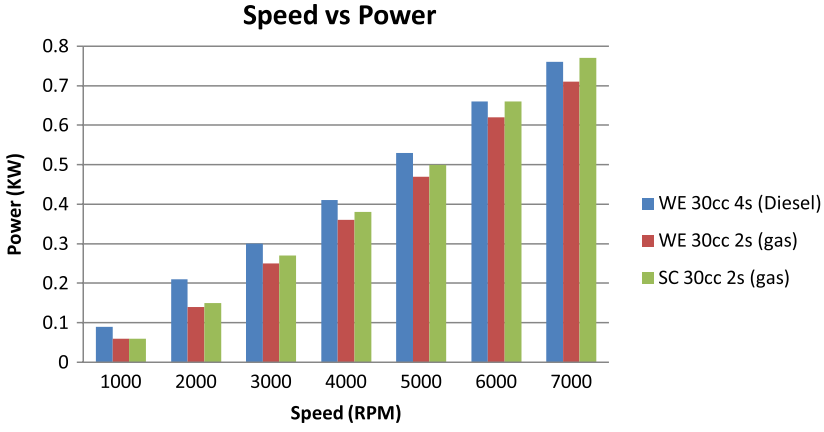

Figure 13. Power comparison of Wiseman diesel, gas, and a conventional slider-crank gas engines.

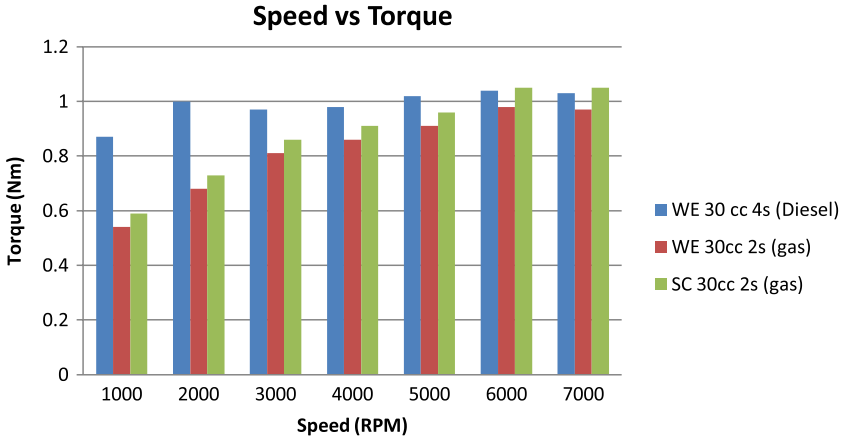

Figure 14. Torque comparison of Wiseman diesel, gas, and conventional slider-crank gas engines.

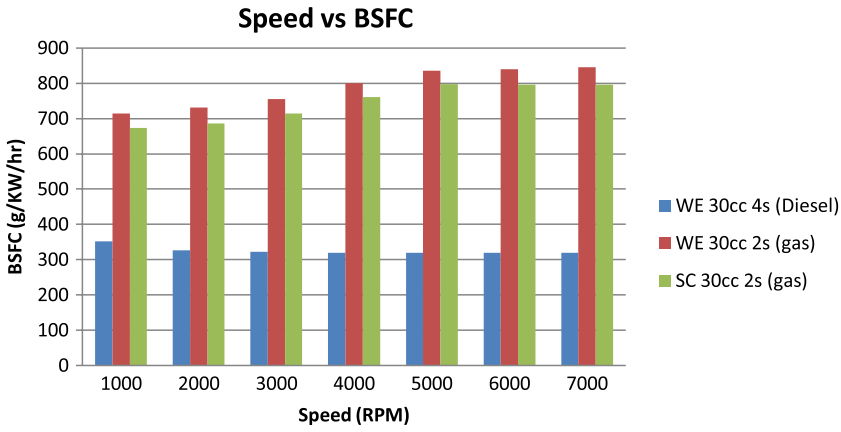

Figure 15. Fuel efficiency comparison of Wiseman diesel, gas, and conventional gas engines.

Table 5. Performance summary at the peak speed of 7,000 rpm

Engine	Power (KW)	Torque (Nm)	BSFC (g/KW/h)
Wiseman two-stroke (gas)	0.71	0.97	845.08
Wiseman four-stroke (diesel)	0.76	1.03	319.62
Slider-crank two-stroke (gas)	0.77	1.05	796.2

cylinder head with contra piston acting as the bottom face of the combustion chamber. By adjusting the distance travelled by the contra piston with the help of a bolt, the effective cylinder clearance volume can be changed. This results in change of the compression ratio. The ability to change the compression ratio of the engine allows it to operate on variety of fuels without knocking. The modified cylinder head and the contra piston design can be seen in Figure 16 below.

An approach similar to the diesel engine model was adopted to simulate the VCR Wiseman UAV engine. Since the contra piston design only changes the compression ratio of the engine, the software model for the two-stroke Wiseman engine (alpha prototype) was kept unchanged except for the compression ratio. A simulation was carried out to analyze the performance of the Wiseman engine while operating on Ethanol (E85) fuel. E85 is a blend of gasoline and ethanol, with 85% ethanol and 15% gasoline by volume. It is also known as flex-fuel (US Department of Energy, Energy Efficiency & Renewable Energy, 2013). It has a higher octane rating than gasoline and is believed to produce more power. Studies have shown an increase of about 5% output power by adding 10%

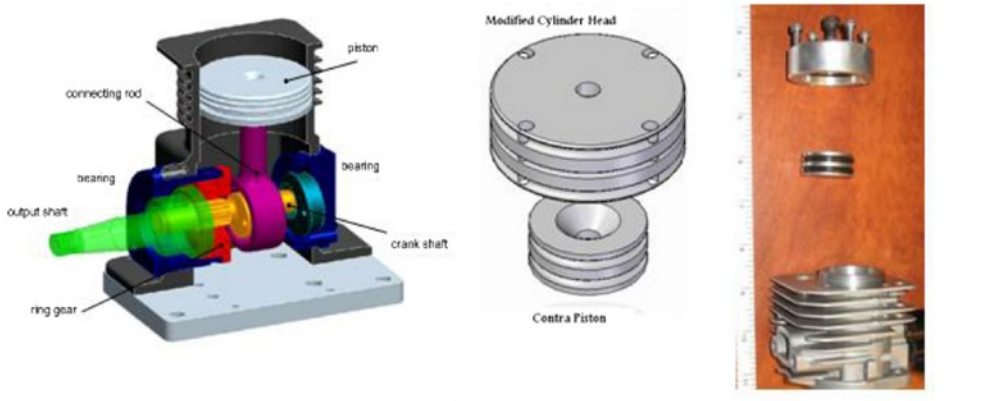

(a) Wiseman engine (b) contra Piston Model (c) Contra Piston prototype

Figure 16. Variable compression Wiseman UAV engine.

ethanol blend in a spark ignited combustion engine (Datta, Chowdhuri, & Mandal, 2012). Increasing the concentration of the ethanol in the fuel blend also tends to increase the output power and the overall efficiency (Celik, 2007). The fuel properties of E85 considered for the simulation can be seen in Table 6 below.

Studies have shown that spark-ignited engines, while operating on ethanol blends, performed better at a compression ratio of about 12:1 to 13:1 (Costa & Sodre, 2010a). So the compression ratio in the software model for the Wiseman engine was changed to 12:1 while simulating its performance on E85 fuel. The engines utilizing ethanol have a higher BSFC, since ethanol has a lower calorific value than gasoline. This means that the engine consumes more fuel to generate the same amount of power and torque while running on ethanol, as compared to gasoline (Costa & Sodre, 2010b).

From comparing the results of the engine operating on gasoline and E85 in Figure 17, it can be noticed that the Wiseman engine produced less or identical power at lower speeds. But at the peak speed of 7,000 rpm, the output power of the engine was 1.4% more in the case of E85 as opposed to gasoline. This is typical of a port-inject gasoline engine operating on ethanol (Cahyono & Bakar, 2010). Another reason for higher power output while using E85 in the Wiseman UAV engine is because, at higher temperatures, ethanol has a better thermal efficiency than gasoline as ethanol has a higher heat of vaporization. When the compression ratio is increased, the engine burns a richer mixture of air–fuel in the case of E85, resulting in a higher output power (Costa & Sodre, 2010a).

From Figure 18, it can be noticed that the torque generated by the Wiseman UAV engine while operating on E85 is slightly higher. As mentioned earlier, this is because it had richer air–fuel which causes the fuel to burn closer to stoichiometric, resulting in a better combustion (Topgül, Yücesu, Çinar, & Koca, 2006). The simulated results for WHE running on E85 showed that an increase in

Table 6. E85 fuel properties (US Department of Energy, Energy Efficiency & Renewable Energy, 2013)

Fuel properties of E85	
Fuel system	Direct injected
Fuel type	Ethanol
Calorific value (kJ/kg)	2,8765
Density (kg/l)	0.782
H/C ratio fuel (molar)	2.7177
O/C ratio fuel (molar)	0.3951
Molecular mass (kg/k mol)	46
Maldistribution factor	1.000

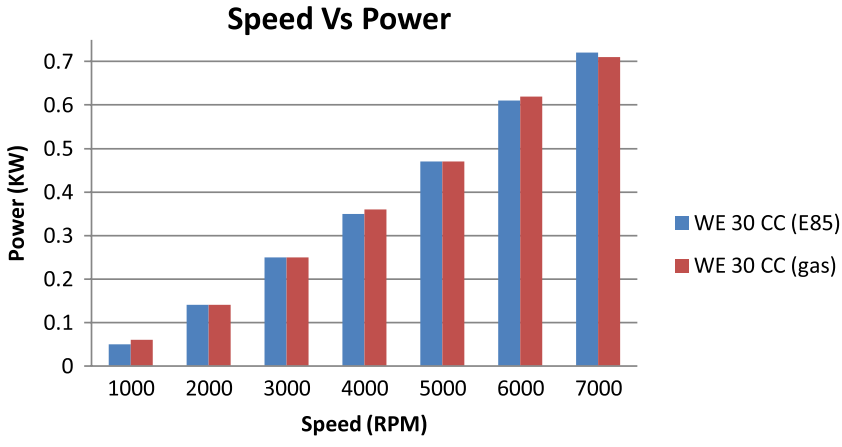

Figure 17. Power comparison of Wiseman engine with contra piston (E85 and gas).

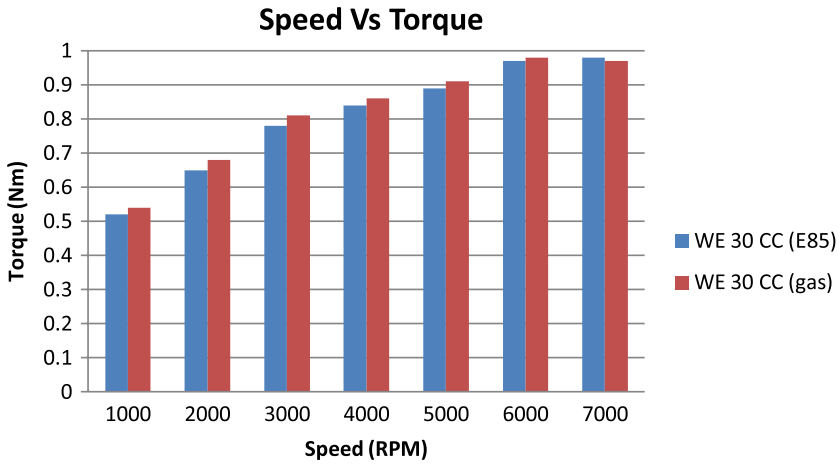

Figure 18. Torque comparison of Wiseman engine with contra piston (E85 and gas).

torque is only at the peak RPM, because at lower RPMs, the high calorific value of gasoline results in higher torque. As the engine speed increased, the ethanol blend tends to produce more torque due to its faster flame velocity. The higher compression ratio used for E85 fuel also increased the cylinder brake mean effective pressure (BMEP), so more work was done on the piston causing an increase in the output torque (Costa & Sodre, 2010b).

Studies have shown that increasing the concentration of ethanol by 10–20% in an ethanol–gasoline blend reduced the calorific value of the fuel, which caused an increase in fuel consumption (Cahyono & Bakar, 2010). In other words, more fuel is required for an engine operating on E85 blend to do the same amount of work as an engine running on pure gasoline. This trend in fuel efficiency is also evident in the results generated by the LES software. The comparison of the results in Figure 19 shows that the Wiseman UAV engine, when running on E85, tends to consume more fuel at every speed with an increase of almost 41.5% at the peak RPM (Table 7).

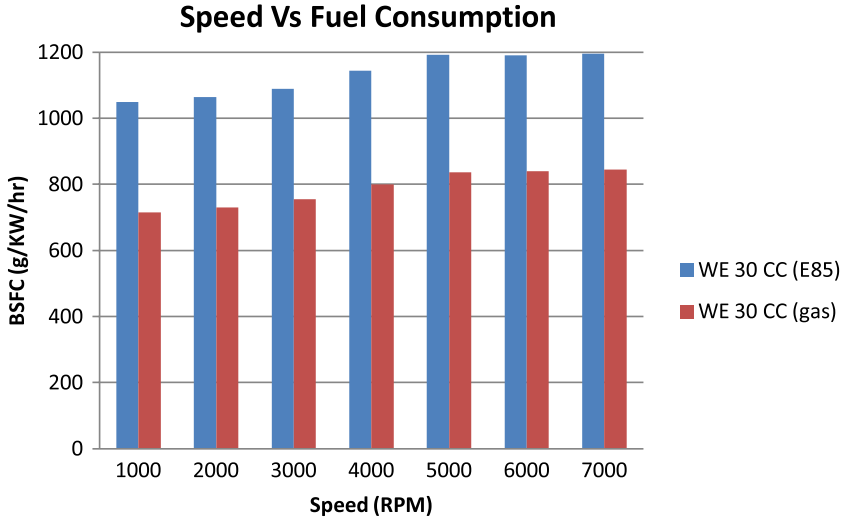

Figure 19. Fuel consumption comparison of Wiseman engine with contra piston (E85 and gas).

Table 7. Performance summary of Wiseman with contra piston (E85 and gas) at 7,000 rpm

Engine	Power (KW)	Torque (Nm)	BSFC (g/KW/hr)
Wiseman UAV (gas)	0.71	0.97	845.08
Wiseman UAV (E85)	0.72	0.98	1,196.21

3.1. Scaling the Wiseman engine prototypes with respect to engine size

There is a need to increase the engine size of the Wiseman engine in order to expand its range of applications. The current 30cc Wiseman alpha prototype engine was designed to produce 0.99 HP, whereas engines required for electric generators, lawn mowers, UAVs, and small tractors need to produce power output much higher than 1 HP. For this purpose, a series of theoretical Wiseman prototypes were designed and their performance was simulated in LES software. These engines were also simulated using conventional slider-crank for comparison. The new theoretical prototypes were designed to produce 10, 20, and 30 HP (7.46, 14.91, and 22.37 KW, respectively). Furthermore, analysis was conducted to determine how the engine's performance varied with respect to its size, and while operating on different fuels (gasoline, diesel, and ethanol).

The engines were designed to have the following characteristics:

- Single cylinder, with a four-stroke combustion cycle, and a peak performance speed of 2,000 rpm.
- Compression ratio of 8:1 was chosen for the gasoline engines, 16:1 for diesel engines, and 13:1 for ethanol engines.
- Indicated Mean Effective Pressure (IMEP) of 0.7 MPa.
- Mechanical efficiency (η_{mech}) of 80%.
- BMEP of 0.56 MPa (IMEP $\times$ η_{mech}).
- Bore/stroke ratio (L/D) of 1.2 for gasoline and ethanol engines and 1.25 for diesel engines.
- The gasoline and ethanol engines used a carburetor and the diesel engines were direct injected.

The following steps further explain the calculations carried out during the designing process of each prototype:

(i) Taking the above-mentioned specifications into consideration, the engine bore diameter was calculated by:

$$\mathrm{Bp} = \mathrm{BMEP} \times L \times A \times N \tag{7}$$

where Bp is the Brake horsepower in Watts; BMEP is the brake mean effective pressure; L is the stroke length ($1.2 \times D$); A is the area of the bore $\left(\frac{\pi}{4}D^2\right)$; N is the engine speed (Max. RPM/2).

This step was carried out to calculate the bore diameter for each engine, and their respective stroke lengths were found.

(ii) Once the bore diameter and the stroke length was found, the engine swept volume was calculated by using:

$$Vs = A \times L \tag{8}$$

where Vs is the cylinder swept volume; A is the area of the bore $\left(\frac{\pi}{4}D^2\right)$; L is the stroke length.

(iii) Finally, torque at peak performance RPM for each engine was calculated;

$$T = \frac{\mathrm{HP} \times 5252}{\mathrm{Speed}} \tag{9}$$

where the horsepower (HP) is in Kilowatts (KW) and the speed at the peak performance RPM of 2,000.

3.2. Scaling laws for ICEs

Now, to analyze the performance of these prototypes, and predict how their output changes with respect to the size, some performance scaling laws were established. Since every engine's

performance parameters vary over its operating range, comparing them at randomly selected points would not draw any meaningful conclusions. In order to compare the performance metrics across different engines, the engines needed to be compared at constant speed (2,000 rpm) and air–fuel ratio. Using this method, the performance can be isolated and treated as a result of change in engine size. The scaling laws were based on the laws proposed by Dr. Shyam Kumar Menon over the years of his research in engine scaling. More than 40 engines, single cylinder to 36 cylinders, and displacement ranging from 0.1cc to almost 100,000cc, were studied and tested by Dr. Menon to establish trends in the engine output based on their displacement. The following scaling laws were proposed by Menon (2010):

I. Scaling the bore and stroke of the engine

The engines with displacement less than 1,000cc are likely to have a "square" design with a few exceptions between the ranges of 1,000–8,000cc as shown in Figure 20. This meant that the bore-to-stroke ratio for those engines is close to 1. But as the engines got closer to a displacement of 1,000cc, the design changed to slightly "under squared" (Menon, 2010).

The calculated displacements of the Wiseman prototypes and its corresponding bore-to-stroke ratios in Tables 8 and 9 were plotted to verify the established scaling law. It can be seen from Figure 20 that the engines tend to have a bore-to-stroke ratio closer to 1, regardless of their displacement.

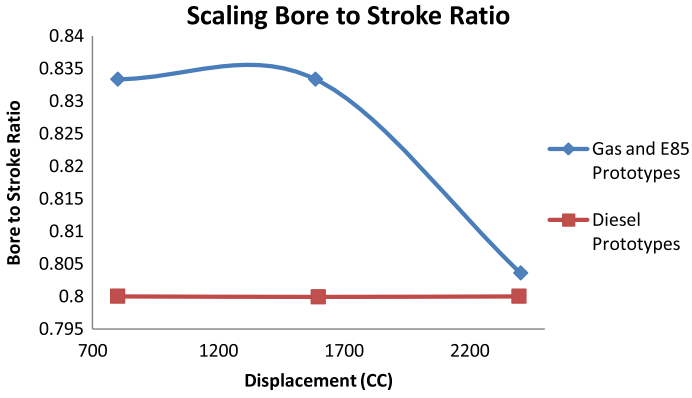

Figure 20. Scaled relationship between engine sizes and bore-to-stroke ratio.

Table 8. Summary calculated specifications for 10, 20, and 30 HP gasoline engines

Engine power (KW)	Bore diameter (mm)	Stroke length (mm)	Swept volume (l)	Calculated torque (Nm)	Bore-to-stroke ratio	Swept volume (cc)
7.46	94.7	113.64	0.800	35.6	0.83333	800
14.914	119	142.8	1.587	71.21	0.83333	1,587
22.371	135	168	2.404	106	0.80357	2,404

Table 9. Summary of calculated specifications for 10, 20, and 30 HP diesel engines

Engine power (KW)	Bore diameter (mm)	Stroke length (mm)	Swept volume (l)	Calculated torque (Nm)	Bore-to-Stroke ratio	Swept volume (cc)
7.46	93.4	116.75	0.7995	35.6	0.8	799.5
14.914	117.65	147.063	1.598	71.21	0.7999	1,598
22.371	134.68	168.35	2.397	106	0.8	2,397

Notes: An approach similar to designing the Wiseman UAV engine with contra piston was taken for ethanol engines. This meant that only the compression ratio (13:1) and fuel properties (E85) were changed in the LES models of gasoline engines.

This is especially true for the diesel engine prototypes. One reason behind this could be that the data-set used to test this particular scaling law was too small to draw any meaningful conclusion. Though, the Wiseman diesel prototypes showed a strong relationship with the Kohler diesel engines and the Ford automobile engines tested between the ranges of 700–3,000cc (approximately) (Menon, 2010).

II. Scaling the engine peak torque at peak power output

It was established that the engine torque at peak power increases with the increase in engine displacement (Menon, 2010). The output torque results generated by software simulations at peak power for each engine prototype was plotted to verify this relationship.

As seen in Figure 21, the Wiseman engines have shown increase in torque as the cylinder displacement increased. The trend has a strong correlation ($R^2 > 0.99$), and so the torque seems to be directly proportional to the displacement. As the cylinder displacement of the Wiseman engine increases, the output toque also increases. The Wiseman engine is known to produce lower torque compared to a slider-crank engine of the same size because of its longer stroke length. But in the Wiseman engine as the side loads is negligible, the decrease in torque is compensated by its lowered cylinder friction. Thus, the net torque at output shaft is more.

Once again, the same trend can be noticed in the case of slider-crank engines, from Figure 22. Similar to the Wiseman engines, the output torque of the slider-crank engines also increase as the engine displacement increases. Slider-crank engines running on gasoline, E85, and diesel produce more torque as engine displacement is increased.

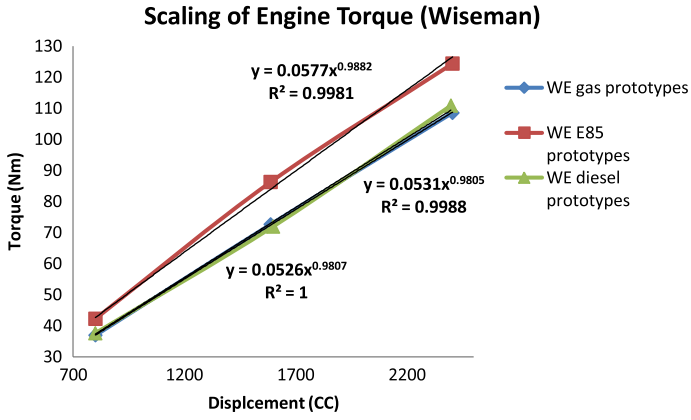

Figure 21. Scaling Wiseman engine's torque with engine size at 2,000 rpm.

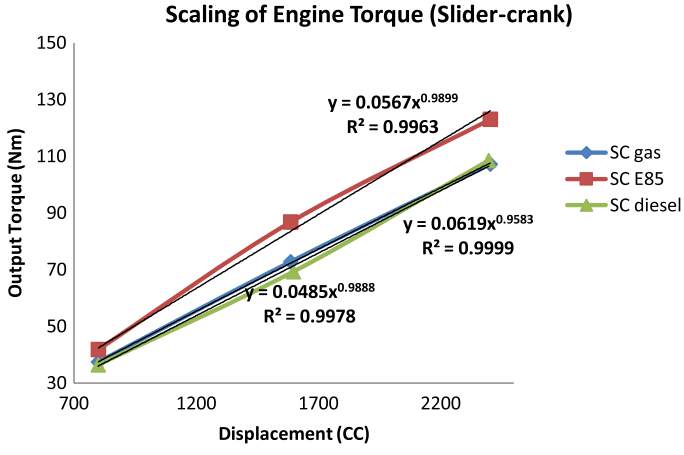

Figure 22. Scaling slider-crank (SC) engine's torque with engine size at 2,000 rpm.

Figure 23 shows a comparison of the output torque of the Wiseman engines and slider-crank engines of the same size, while operating on different fuels. It can be seen that as the engine displacement increased, the Wiseman prototypes produced *slightly more torque* than similar slider-crank engines. The original 30cc Wiseman engine produced less torque than the slider-crank engine because its piston was set higher, providing less combustion volume.

III. Scaling the engine peak power output

Similar to the relationship between torque and displacement, the peak output power of the engine also increased as the engine's combustion volume increased. Though, the change in output power with respect to the displacement was more for the two-stroke engines than the four-stroke engines. It has been theoretically known that the two-stroke engines tend to produce more power per unit displacement (Menon, 2010).

Figure 24 confirms this relationship as it can be seen that the output power of the engine, as a function of the engine displacement, increased as the displacement increased. This is true irrespective of the fuel being used. Figure 25 shows that this is also true for the slider-crank engines of same size. Though, the curves do not follow the same shape and trend as the Wiseman engines. Thus, it can be noted that the Wiseman engines produced more power than the slider-crank engines of the same size.

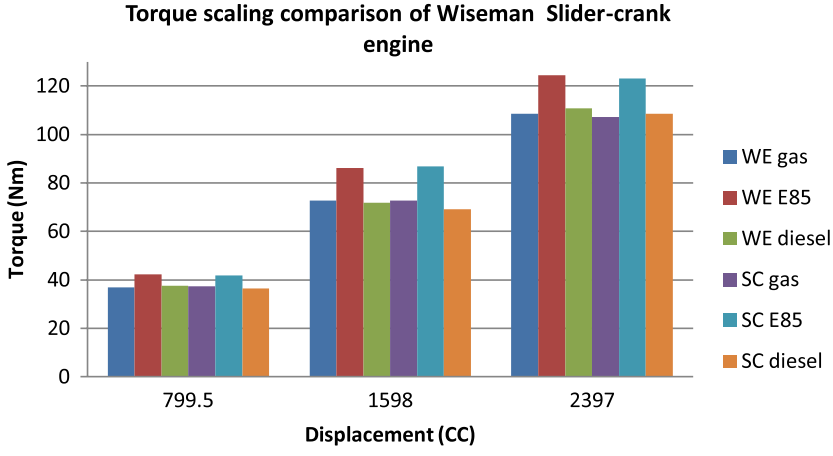

Figure 23. Comparing the scaled torque of Wiseman (WE) and slider-crank (SC) engine.

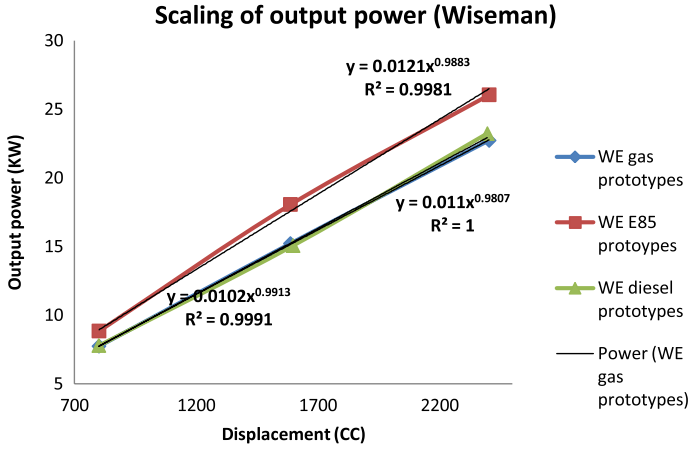

Figure 24. Scaling Wiseman engine's peak power with size at 2,000 rpm.

When comparing the power generated by the Wiseman engine and the slider-crank engine of similar displacements, *it was noticed that the Wiseman variants produced more power than its slider-crank counterparts irrespective of the fuel type*. This can be seen in Figure 26. This was especially true for the 30 HP (2,397cc) Wiseman engine operating on E85.

IV. Scaling the engine fuel consumption at peak power output

The miniature engines that Dr. Menon tested showed decrease in fuel efficiency as the size of the engine decreased. This was due to increase in motoring loses when the engine components were scaled down. Though, for the engines of moderate-to-large sizes, the fuel efficiency increased with increase in displacement. The change in this trend was found after the ranges of 15–20cc (Menon, 2010).

As seen in Figure 27, the Wiseman prototypes showed similar trend, but not with strong correlation considering the lower values of R^2. It can be seen that the fuel efficiency varies with the change in the displacement but overall, there is a slight improvement with increase in the engine displacement. Similar to the results from previous multi-fuel tests, the E85 engines in general consume more fuel than the gas and diesel variants. This could again be due to the lower calorific value of the E85 fuel. Again, the diesel Wiseman engines are most fuel efficient, with the 30 HP variant having the highest efficiency. It was also noticed that the gas variants did not show any significant change in the fuel efficiency with change in displacement.

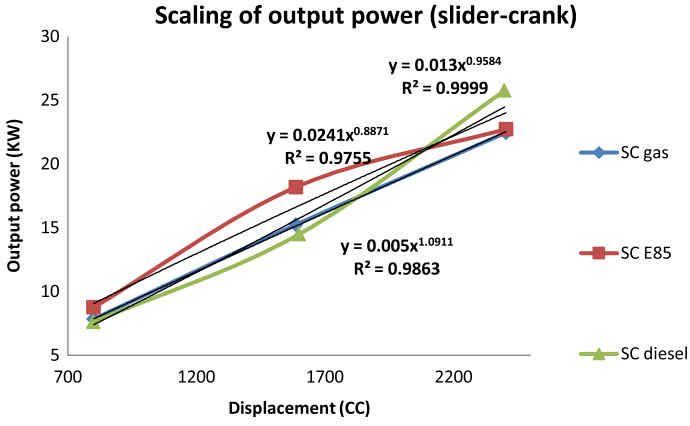

Figure 25. Scaling slider-crank engine's peak power with size at 2,000 rpm.

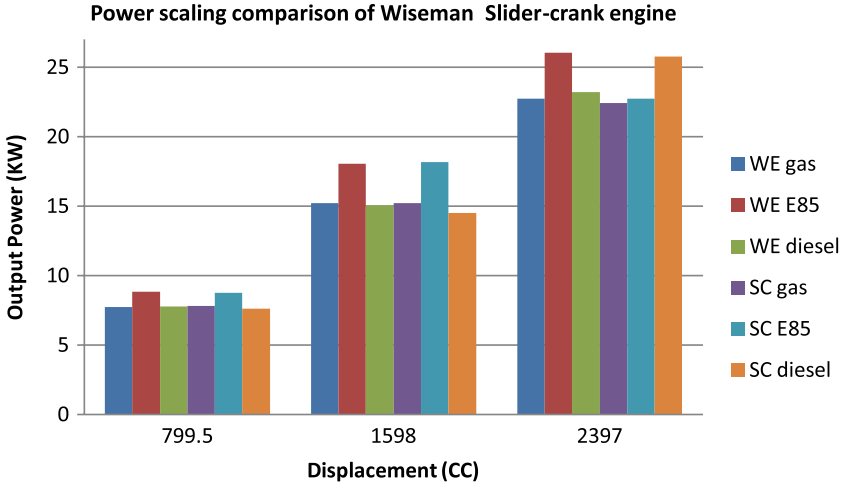

Figure 26. Comparing the scaled power of Wiseman and slider-crank engine.

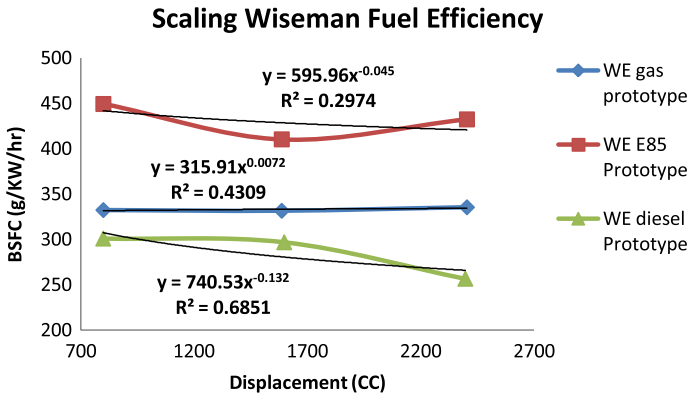

Figure 27. Scaling Wiseman engine's BSFC with respect to engine displacement.

When it comes to the slider-crank versions of the engines, the trend remained the same, but they had slightly lower fuel consumption as the engine displacement increased as shown in Figure 28. This observation was further compared to see how the engines with Wiseman mechanism perform in terms of fuel efficiency when compared to the slider-crank versions of the same size.

By comparing the BSFC results of both the mechanisms in Figure 29, it can be seen that the Wiseman engines tend to be slightly less fuel efficient but the difference is minor. However, both the engines follow a common trend, that is, increase in fuel efficiency with increase in the engine

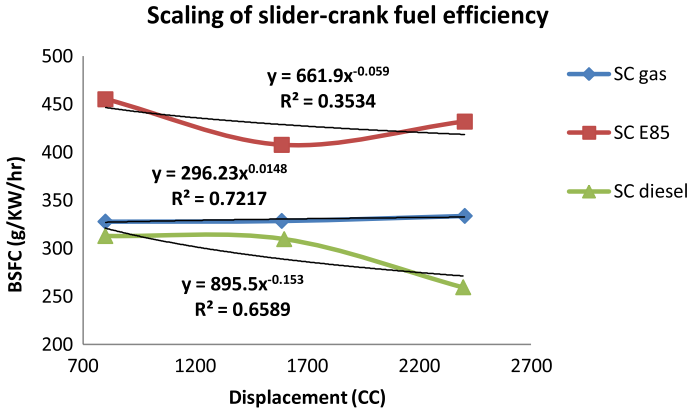

Figure 28. Scaling slider-crank engine's BSFC with respect to engine size.

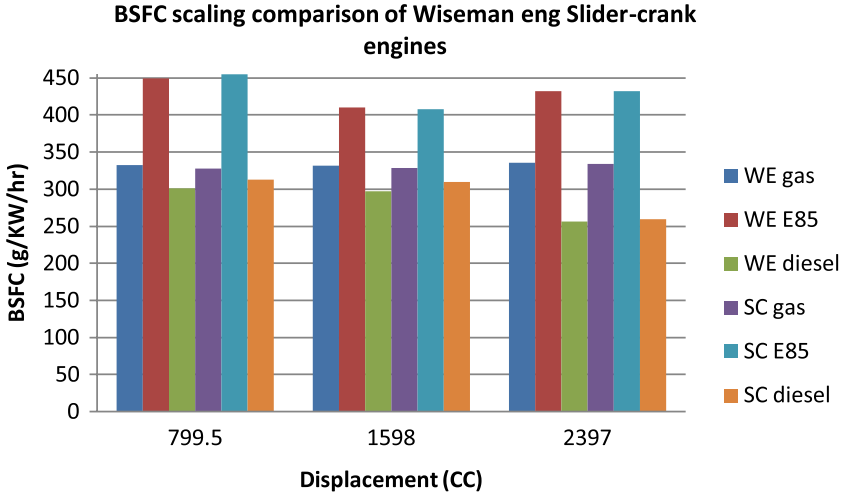

Figure 29. Comparing the scaled BSFC of Wiseman and slider-crank engine.

displacement. The gas and E85 variants of both the engines have almost identical fuel consumption, whereas the Wiseman diesel engines prove to be a slightly more fuel efficient than its slider-crank counterparts.

V. Scaling the engine BMEP

Another important engine parameter to gage the engine's performance is the BMEP. The BMEP decides the work done by the piston, which in turn determines the output torque and power. This reflects on the overall quality of the engine design. It was established that the engine BMEP gradually increases with increase in engine displacement, in majority of the cases (Menon, 2010).

The results in Figure 30 show a similar trend in the peak BMEP of the Wiseman engines. Although the trend is not clearly recognizable due to the small size of the data-set, overall the BMEP seems to increase with increase in cylinder displacement. The established scaling law seems most evident in the gas variants of the engines, whereas the diesel engines tend to show the opposite pattern. Also, the engines operating on E85 fuel produced more BMEP than the gas versions in general, with the 30 HP engine having the highest BMEP output. This pattern was also evident while comparing the performance of the Wiseman 30cc engine operating on gas and E85. Though, the 20 HP ethanol engine had a lower cylinder BMEP than the 20 HP diesel engines.

While scaling the slider-crank versions of the same engines, a different trend was noticed as shown in Figure 31. The engines operating on gas and E85 had a gradual increase in the cylinder BMEP, while the diesel variants followed a trend more similar to the E85 version of the Wiseman engine. Though, the ethanol engines still produce higher BMEP than the gas counterparts. And, the 30 HP version of the diesel engine produces highest BMEP of them all.

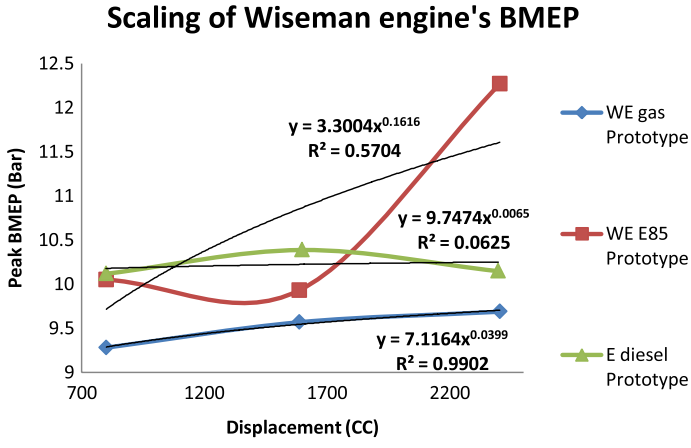

Figure 30. Scaling Wiseman engine's BMEP with respect to engine displacement.

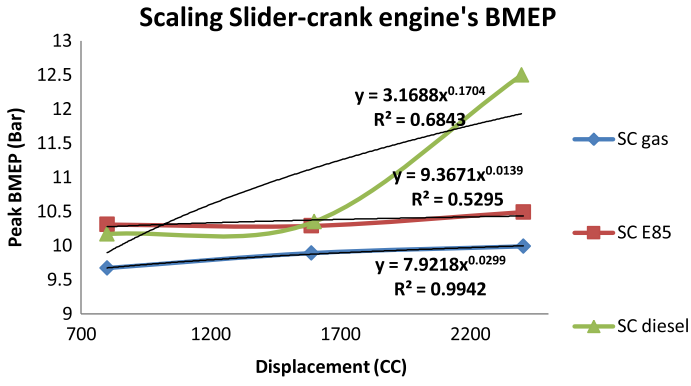

Figure 31. Scaling slider-crank engine's BMEP with respect to engine size.

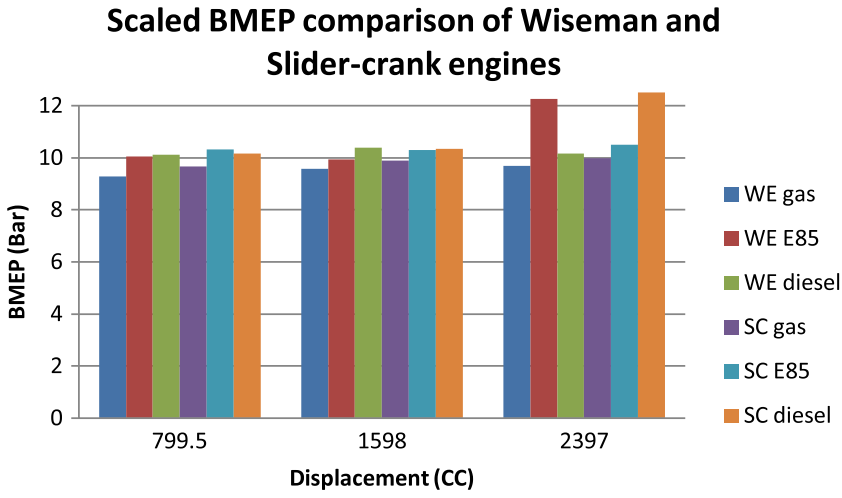

Figure 32. Comparing the scaled BMEP of Wiseman and slider-crank engine.

After comparing the BMEP results of the Wiseman and slider-crank engines in Figure 32, it was observed that slider-crank engines have a higher BMEP than the Wiseman engines in general. There are two exceptions to this trend, and both are for the 30 HP variants of these engines. The 30 HP slider-crank diesel and 30 HP Wiseman ethanol variants produce almost identical BMEP. The BMEP of these two engines is also the highest among all the other engines.

4. Conclusion

In this research, performance of the WHE was examined with respect to power output, torque, and BSFC and compared to similar slider-crank engines. The WHE was modeled in LES using a user-defined subroutine that simulated the hypocycloid mechanism. WHE alpha prototype was modeled and simulated in LES. This prototype was also tested using a dynamometer. The LES simulation results and dynamometer results were comparable and showed similar trend.

Furthermore, a four-stroke diesel version of the Wiseman engine was modeled in the LES software. The simulation results for this engine were promising in almost all aspects. It was seen that this engine produced higher power and torque than the two-stroke Wiseman and slider-crank engines running on gas.

The multi-fuel capability of the Wiseman engine with contra piston was also studied which showed that compared with gasoline, it produced higher power and torque while operating on E85 flex-fuel. To understand the effect of scaling on WHE, four-stroke Wiseman engines were designed to produce 10, 20, and 30 HP, and performance analysis was conducted to predict how the output power, torque, and fuel efficiency would change according to the displacement while operating on different fuels. Overall, it was noticed that the Wiseman engines fared better in terms of power and torque than the slider-crank engines as its size increased. A similar trend was also noticed when fuel consumption was studied. As the Wiseman engine's displacement increased, it was found to be more fuel efficient due to reduced motoring losses in it. It was found that the 30 HP Wiseman engine, while operating on diesel, had the best fuel efficiency. This trend in increased performance with increase in displacement was also true for the cylinder BMEP.

The scaling and multi-fuel analysis suggested that four-stroke diesel and ethanol variants of the Wiseman engine were very promising compared to the two-stroke gasoline engines. Currently, work is underway to prototype Wiseman engines studied in this research. Later, these engines will be tested using a dynamometer and experimental results will be compared with the simulations presented in this paper.

Funding
This research was partially supported by the funding from Science Foundation Arizona and Wiseman Technologies Incorporated.

Author details
Priyesh Ray[1]
E-mail: priyesh.ray@asu.edu
Sangram Redkar[1]
E-mail: sredkar@asu.edu
[1] Department of Engineering, Arizona State University, Mesa, AZ 85212, USA.

Citation information
Cite this article as: Analysis and simulation of Wiseman hypocycloid engine, P. Ray & S. Redkar, *Cogent Engineering* (2014), 1: 988402.

References

Andriano, M. B. (1998). *Design, construction and testing of hypocycloid machines.* Detroit: SAE International.
Annand, W. J. D. (1963). Heat transfer in the cylinders of reciprocating internal combustion engines. *Archive: Proceedings of the Institution of Mechanical Engineers 1847–1982 (vols 1–196), 177*, 973–996. doi:10.1243/PIME_PROC_1963_177_069_02
Beachley, N. H., & Lenz, M. A. (1988). *A critical evaluation of the geared hypocycloid mechanism for internal combustion engine application*. Detroit, MI: Society of Automotive Engineers. http://dx.doi.org/10.4271/880660
Cahyono, B., & Bakar, R. A. (2010). Effect of ethanol addition in the combustion process during warm-ups and half open throttle on port-injection gasoline engine. *American Journal of Engineering and Applied Sciences, 4*, 66–69. doi:10.3844/ajeassp.2011.66.69
Celik, M. B. (2007). Experimental determination of suitable ethanol–gasoline blend rate at high compression ratio for gasoline engine. *Applied Thermal Engineering, 28*, 396–404. doi:10.1016/j.applthermaleng.2007.10.028
Conner, T. (2011). *Critical evaluation and optimization of a hypocycloid Wiseman engine* (Master's thesis). Arizona State University, Mesa, AZ.
Costa, R. C., & Sodre, J. R. (2010a). Compression ratio effects on an ethanol/gasoline fuelled engine performance. *Applied Thermal Engineering, 21*, 278–283.
Costa, R. C., & Sodre, J. R. (2010b). Hydrous ethanol vs. gasoline–ethanol blend: Engine performance and emissions. *Fuel, 89*, 287–293. http://dx.doi.org/10.1016/j.fuel.2009.06.017
Datta, A., Chowdhuri, A. K., & Mandal, B. K. (2012). Experimental study on the performances of spark ignition engine with alcohol–gasoline blends as fuel. *International Journal of Energy Engineering, 2*, 22–27.
Ganesan, V. (2012). *Internal combustion engines* (4th ed.). New Delhi: Tata McGraw.
Hatz Diesel. (2012). *Operator's manual: Diesel engines*. Germany. Retrieved July 21, 2014, from http://www.hatz-diesel.com/uploads/tx_hatzproducts/BA_1B_EN_43380210.pdf
Ishida, K., & Matsuda, T. (1975). Fundamental researches on a perfectly balanced rotation–reciprocation mechanism. *Bulletin of the JSME, 18,* 185–192.
Karhula, J. (2008). *Cardan gear mechanism versus slider crank mechanism in pumps and engines*. Lappeenranta: Lappeenranta University of Technology.
Menon, S. (2010). *The scaling of performance and losses in miniature internal combustion engines* (Doctoral dissertation). University of Maryland, College Park, MD.
Ruch, D. M., Fronczak, F. J., & Beachley, N. H. (1991). 911810 —Design of a modified hypocycloid engine. *SAE International,* 73–89.
Special plane curves. (2005–2014). Retrieved July 21, 2014, from http://www.math10.com/en/geometry/analytic-geometry/geometry5/special-plane-curves.html
Topgül, T., Yücesu, H. S., Çınar, C., & Koca, A. (2006). The effects of ethanol–unleaded gasoline blends and ignition timing on engine performance and exhaust emissions. *Renewable Energy, 31*, 2534–2542. http://dx.doi.org/10.1016/j.renene.2006.01.004
US Department of Energy, Energy Efficiency & Renewable Energy. (2013). *Handbook for handling, storing, and dispensing e85 and other ethanol–gasoline blends*. Retrieved July 21, 2014, from http://www.afdc.energy.gov/uploads/publication/ethanol_handbook.pdf
Wiseman, R. (2001). *US Patent No. 6,510,831*. Waveland, MS: US Patent and Trademark Office.
Wiseman Engine Group. (2010). *The engine of the future-today!* Pass Christian, MS: Business Plan.
Wiseman Technologies Inc. (n.d.). Retrieved July 21, 2014, from http://www.wisemanengine.com/AUVSIWisemanPaPer.doc